

# Photoemission Studies of Copper and Silver: Theory\*†

C. N. BERGLUND‡ AND W. E. SPICER

*Stanford Electronics Laboratories, Stanford University, Stanford, California*

(Received 22 June 1964)

Theoretical expressions are derived for the quantum yield and for the energy distribution of photoelectrons assuming bulk photoemission from a solid. The effects of electrons which escape without inelastic scattering after optical excitation, and of those electrons which escape after one inelastic-scattering event, are considered. The expressions relate optical transition probabilities, optical constants, and mean free paths for inelastic scattering in a solid to quantities which can be measured in photoemission experiments. Examples of photoemission data are interpreted to show how the contribution of once-scattered electrons can be separated from the contribution of those electrons which have not suffered an inelastic-scattering event before escaping. The contribution to photoemission of those electrons which have not been scattered is analyzed to show the way in which direct and nondirect optical transitions can be identified and the way in which the density of states in a solid can be determined. The contribution of once-scattered electrons to photoemission is analyzed to show the way in which the nature and strength of inelastic-scattering mechanisms can be determined. The effects of electron-electron scattering, scattering by plasmon creation, and the Auger process are described, and methods of obtaining mean free paths and other scattering parameters are suggested.

## I. INTRODUCTION

**P**HOTOEMISSION from solids is a two-step process. Electrons are first optically excited into states of higher energy; then they move to the surface of the solid, with or without scattering, and escape into vacuum. As a result, measurements of the spectral distribution of the photoelectric yield, and of the energy distribution of photoemitted electrons at individual photon energies, can be used to study both the optical excitation processes and the electron-scattering processes in solids. The main purposes of this paper are to explain how the effects of electrons which escape after one or more inelastic-scattering events can be separated from the effects of those which escape without significant inelastic scattering in photoemission, and to outline methods by which the data can be interpreted in terms of band structure, optical excitation probabilities, and scattering probabilities.

In the past, photoemission has been considered by many authors.<sup>1-3</sup> However, the emphasis has been on the details of this phenomenon at photon energies near the threshold. In this paper, photoemission at photon energies well above the threshold is emphasized. The effects of inelastic scattering are taken into account by considering only those electrons which escape without inelastic scattering and those which escape after one inelastic scattering. By this means, general results are obtained which allow detailed interpretation of photoemission data.

In parts A, B, and C of Sec. II, an expression for the energy distribution of photoemitted electrons at a

given photon energy is derived considering only electrons which escape without inelastic scattering and electrons which escape after one inelastic scattering. This expression is related to the optical transition probabilities in the solid and the optical constants in part D. In parts E and F the effects of electron-electron scattering, of electron scattering by plasmon creation, and of the Auger process are considered. Section III gives an expression for the photoelectric quantum yield, and explains in detail the factors affecting it. Using the expressions for electron energy distribution and quantum yield derived in Secs. II and III, typical experimental data are interpreted in Sec. IV. The characteristic effects on the data of direct optical transitions and those transitions which are not direct, of electron-electron scattering, of electron scattering by plasmon creation, and of the Auger process are all discussed in detail.

It will be shown that photoemission data can be used to determine whether an optical transition is direct or not; that is, whether direct conservation of  $k$  vector in an optical transition is required (Sec. IV.A). If it is found that direct conservation of  $k$  vector is not necessary in an optical transition, there are two possible explanations. Either the transition is indirect,  $k$  vector being conserved by some mechanism such as phonons,<sup>4</sup> or conservation of  $k$  vector as a selection rule is not important.<sup>5</sup> No distinction between the two possibilities will be made here. All optical transitions in which direct conservation of  $k$  vector is not important will be referred to as nondirect transitions.

## II. ENERGY DISTRIBUTION OF PHOTOEMITTED ELECTRONS

### A. Probability of Electron Escape Without Inelastic Scattering

Consider an electron excited to some energy  $E$  and momentum  $p$  at a distance  $x$  from the surface of a

\* Work supported by the Advanced Research Projects Agency through the Center for Materials Research at Stanford University, Stanford, California.

† Based on a thesis submitted by C.N.B. to Stanford University in partial fulfillment of the requirements of the Ph.D. degree.

‡ Present address: Bell Telephone Laboratories, Murray Hill, New Jersey.

<sup>1</sup> R. H. Fowler, *Phys. Rev.* **38**, 45 (1931).

<sup>2</sup> L. Apker, E. Taft, and J. Dickey, *Phys. Rev.* **74**, 1462 (1948).

<sup>3</sup> E. O. Kane, *Phys. Rev.* **127**, 131 (1962); G. W. Gobeli and F. G. Allen, *ibid.* **127**, 141 (1962).

<sup>4</sup> L. H. Hall, J. Bardeen, and F. J. Blatt, *Phys. Rev.* **95**, 559 (1954).

<sup>5</sup> W. E. Spicer, *Phys. Rev. Letters* **11**, 243 (1963).

semi-infinite solid as shown in Fig. 1. This electron has just been excited to this state by absorption of a photon. In order for the electron to escape from the solid without any loss of total energy, it must (1) reach the surface of the solid without suffering an inelastic collision, and (2) have a crystal momentum component perpendicular to the photoemitting surface greater than some critical value.

An exact treatment of the scattering and escape problem presents extreme difficulties and will not be attempted here. Rather the following simplifying assumptions will be made:

- (1) The distribution in direction of the excited electrons is isotropic.
- (2) Only inelastic scattering events need be considered.
- (3) The probability of inelastic scattering can be described in terms of a mean free path  $l$ , which is a function only of the electron energy.
- (4) The inelastic scattering is isotropic.
- (5) In order to escape over the surface barrier, the electron must have a component of its total crystal momentum  $p$ , perpendicular to the surface which is greater than some critical value  $p_c$ . The escape probability is assumed to be unity if this condition is satisfied. Since the samples studied consisted of unoriented polycrystals, the first assumption was probably satisfied in a macroscopic sense. The validity of the second assumption is discussed in detail in Sec. II.C.

The third and fourth assumptions cannot be expected to be exact; however, deviations from them would probably not cause first-order errors in the present work. Greater care would have to be taken if measurements were made on single crystals.<sup>3</sup>

The fifth assumption involves the probability of escape of an electron which reaches the surface. As will be seen in the equations derived,  $p$  and  $p_c$  appear only in terms of the form  $(1 - p_c/p)$ . In principle these could be calculated from the known band structure. One effect of elastic scattering will be to scatter electrons into the proper direction for escape. As will be discussed in Sec. II.D, this could be taken into account by redefining the escape probability.

Since these assumptions are not exact, the treatment given here must be considered as only a first approximation.

If  $\theta$  is the angle between the direction of electron momentum upon excitation and the normal to the photoemitting surface as shown in Fig. 1, the electron must move a distance  $x/\cos\theta$  to reach the surface. The probability of the electron escaping without loss of energy following excitation to energy  $E$ , is

$$p_{\text{esc}}(E, x) = \begin{cases} \frac{1}{2} \int_0^{\cos^{-1}(p_c/p)} e^{-x/l \cos\theta} \sin\theta d\theta & \text{if } p \geq p_c, \\ 0 & \text{if } p < p_c, \end{cases} \quad (1)$$

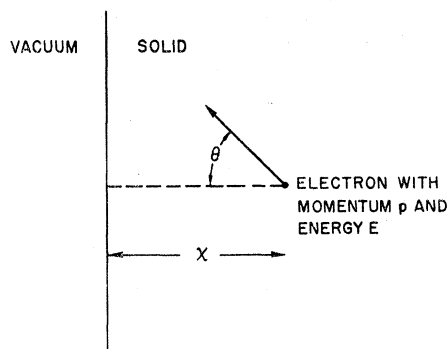


FIG. 1. Definition of terms for bulk photoemission from a solid.  $\theta$  is the angle with the normal and  $x$  is the distance from the surface.

where  $l$  is the mean free path for inelastic-scattering characteristic of electrons with energy  $E$ . Changing variables so that  $z = \cos\theta$

$$p_{\text{esc}}(E, x) = \begin{cases} \frac{1}{2} \int_{p_c/p}^1 e^{-x/lz} dz & \text{if } p \geq p_c \\ 0 & \text{if } p < p_c. \end{cases} \quad (2)$$

This integral does not have a simple closed-form solution. However,  $p_{\text{esc}}(E, x)$  can be used in the integral form, the integration being performed later.

In optical absorption, the rate per unit area at which electrons are excited to energies between  $E$  and  $E + dE$ , in a slab of width  $dx$  located a distance  $x$  from the surface on which the light is incident (see Fig. 1), has the form

$$G(E, x) dE dx = G_0(E) dE e^{-\alpha x} dx, \quad (3)$$

where  $\alpha$  is the absorption coefficient.  $G_0(E)$  will be defined later. From Eqs. (2) and (3), the rate of escape of electrons with energy between  $E$  and  $E + dE$  is

$$R'(E) dE = \int_0^{\infty} p_{\text{esc}}(E, x) G(E, x) dE dx, \quad (4)$$

$$R'(E) dE = G_0(E) dE \int_0^{\infty} p_{\text{esc}}(E, x) e^{-\alpha x} dx.$$

In Eq. (4) the photoemitting solid has been assumed to be semi-infinite to allow the upper limit in the integration to be infinite. Carrying out the integration in Eq. (4) first with respect to  $x$ , integration with respect to  $z$  gives the result:

$$R(E) dE = \frac{G_0(E) dE}{2\alpha} \left\{ 1 - \frac{p_c}{p} \frac{1}{\alpha l} \times \ln \left[ \frac{1 + \alpha l}{1 + (p_c/p)\alpha l} \right] \right\} \begin{cases} p \geq p_c, \\ 0 & p < p_c. \end{cases} \quad (5)$$

This expression is rather difficult to interpret in its

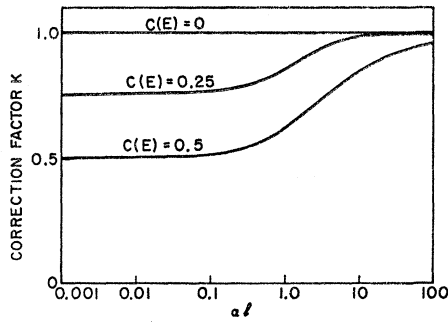


FIG. 2. Values of the correction factor  $K$ .  $\alpha l$  is the product of the absorption coefficient ( $\alpha$ ) and the mean free path for electron scattering ( $l$ ).

present form. It can be written in a form that is more meaningful if the logarithm in Eq. (5) is expanded in an infinite series

$$\begin{aligned} & -\frac{1}{\alpha l} \ln \left[ \frac{1 + \alpha l}{1 + (\rho_c/\rho)\alpha l} \right] \\ & = +\frac{1}{\alpha l} \ln \left\{ 1 - \frac{[1 - (\rho_c/\rho)]\alpha l}{1 + \alpha l} \right\} \\ & = -\frac{1}{\alpha l} \left\{ \frac{[1 - (\rho_c/\rho)]\alpha l}{1 + \alpha l} + \frac{[1 - (\rho_c/\rho)]^2 \alpha^2 l^2}{2(1 + \alpha l)^2} \right. \\ & \quad \left. + \frac{[1 - (\rho_c/\rho)]^3 \alpha^3 l^3}{3(1 + \alpha l)^3} + \dots \right\}. \quad (6) \end{aligned}$$

Substituting Eq. (6) in Eq. (5) and collecting terms gives

$$\begin{aligned} R'(E)dE &= \frac{\frac{1}{2}[1 - (\rho_c/\rho)]G_0(E)dE}{\alpha + (1/l)} \left[ 1 - \frac{[1 - (\rho_c/\rho)]}{2(1 + \alpha l)} \right. \\ & \quad \left. - \frac{[1 - (\rho_c/\rho)]^2 \alpha l}{3(1 + \alpha l)^2} + \dots \right] \quad p \geq \rho_c, \quad (7) \\ &= 0 \quad p < \rho_c. \end{aligned}$$

Equation (7) can be further simplified if a threshold function  $C(E)$  is defined where

$$\begin{aligned} C(E) &= \frac{1}{2}[1 - (\rho_c/\rho)] \quad p \geq \rho_c \\ &= 0 \quad p < \rho_c \end{aligned} \quad (8)$$

and if the infinite series in Eq. (7) (which has a value between  $\frac{1}{2}$  and 1) is represented by a correction factor  $K$ . This correction factor has been evaluated, and plotted as a function of  $C(E)$  and  $\alpha l$  in Fig. 2. Using Eq. (8) and the correction factor  $K$ , Eq. (7) becomes

$$R'(E)dE = \frac{KC(E)G_0(E)dE}{\alpha + (1/l)}. \quad (9)$$

The threshold function  $C(E)$  depends on the crystal momentum  $p$  and the critical crystal momentum for

escape  $p_c$ . As a result, it is a complicated function. However, using Eq. (8), it can be seen that  $C(E)$  is zero for electron energies less than the threshold energy for photoemission, and is 0.5 for electron energies well above threshold.

### B. Probability of Electron Escape After One Inelastic Scattering

In both copper and silver, the effect of electron scattering is small enough over the electron energy range studied (0 to 11.5 eV above the Fermi level) that only those electrons which escape without scattering and those which scatter once before escaping need be considered. The probability of electron escape after scattering once can be derived in a way similar to that for electron escape without scattering.

Consider an electron excited to energy  $E'$  a distance  $x$  from the photoemitting surface as shown in Fig. 3. The probability of this electron escaping with energy between  $E$  and  $E+dE$  after scattering once is the product of three probabilities: (1) the probability that the primary electron will scatter after moving a distance  $r$  in the solid at an angle  $\theta$  with respect to the normal to the photoemitting surface; (2) the probability that this electron will be scattered in this scattering process to an energy between  $E$  and  $E+dE$ ; and (3) the probability that it will escape after the scattering event without further scattering. Referring to Fig. 3, the first probability if the electron velocity direction is random is

$$p_1 = \left[ \frac{1}{2} e^{-r/l'} \sin \theta d\theta \right] (dr/l'), \quad (10)$$

where  $l'$  is the mean free path for inelastic scattering for electrons with energy  $E'$ . The probability of the electron being scattered to an energy between  $E$  and  $E+dE$ ,  $p_2$ , will depend on the scattering mechanism and will be derived for particular cases later. It will be assumed, however, that the electron velocity direction after scattering is random and independent of its initial

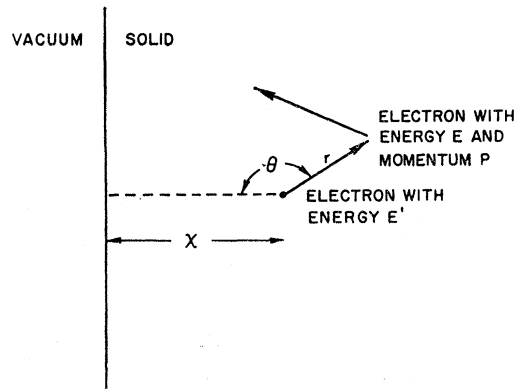


FIG. 3. Definition of terms for photoemission after an inelastic-scattering event.  $r$  is the distance traveled before the inelastic-scattering event.  $E'$  is the energy before scattering.  $E$  and  $p$  are the values of energy and momentum, respectively, after scattering.

velocity. The third probability is given by Eq. (2), where the distance of the electron from the photoemitting surface at the time of the scattering event is  $(x-r\cos\theta)$

$$\begin{aligned} \dot{p}_3 &= \frac{1}{2} \int_{p_c/p}^1 e^{(-x+r\cos\theta)/lz} dz & p \geq p_c, \\ &= 0 & p < p_c. \end{aligned} \quad (11)$$

The probability of an electron escaping after scattering with energy between  $E$  and  $E+dE$  is given by the product of  $\dot{p}_1$ ,  $\dot{p}_2$ , and  $\dot{p}_3$  integrated over all  $r$ ,  $z$ , and  $\theta$ . Referring to Fig. 3, for  $\theta > \pi/2$ , the limits on  $r$  are 0 and  $\infty$ . For  $\theta < \pi/2$ , the upper limit on  $r$  is given by  $r\cos\theta = x$  if it is assumed that an electron with energy  $E'$  which reaches the surface of the photoemitter without scattering escapes with unity probability, and is no longer available to produce electrons with energy  $E$ . Under these conditions, the probability of electron escape after one scattering event is

$$\begin{aligned} \dot{p}_{\text{esc}}''(E', E, x) &= \frac{\dot{p}_2}{4l'} \left[ \int_{\pi/2}^{\pi} d\theta \int_0^{\infty} dr \int_{p_c/p}^1 dz e^{-r/l'} \right. \\ &\quad \times e^{(-x+r\cos\theta)/lz} \sin\theta + \int_0^{\pi/2} d\theta \int_0^{x/\cos\theta} dr \\ &\quad \left. \times \int_{p_c/p}^1 dz e^{-r/l'} e^{(-x+r\cos\theta)/lz} \sin\theta \right]. \end{aligned} \quad (12)$$

Changing variables so that  $y = \cos\theta$ , and integrating Eq. (12) over  $r$ , gives

$$\begin{aligned} \dot{p}_{\text{esc}}''(E', E, x) &= \frac{\dot{p}_2}{4l'} \left[ \int_{-1}^0 dy \int_{p_c/p}^1 dz \frac{e^{-x/lz}}{(1/l') - (y/lz)} \right. \\ &\quad \left. + \int_0^1 dy \int_{p_c/p}^1 dz \frac{(1 - e^{-x/l'y + x/lz}) e^{-x/lz}}{(1/l') - (y/lz)} \right]. \end{aligned} \quad (13)$$

Electrons are excited to energy  $E'$  according to Eq. (3), so the rate of escape of electrons after scattering once with energy between  $E$  and  $E+dE$  is

$$R''(E', E) dE dE' = \int_0^{\infty} [G_0(E') dE' e^{-\alpha x} \times \dot{p}_{\text{esc}}''(E', E, x) dx]. \quad (14)$$

Substituting Eq. (13) in Eq. (14) and carrying out the integrations over  $x$  and  $y$  gives

$$\begin{aligned} R''(E', E) dE dE' &= \frac{\dot{p}_2 dEG_0(E') dE'}{4} \\ &\quad \times \int_{p_c/p}^1 \left[ \frac{1}{\alpha l'} \ln(1 + \alpha l') + \frac{lz}{l'} \ln\left(1 + \frac{l'}{lz}\right) \right] \\ &\quad \times \frac{dz}{\alpha + (1/lz)}. \end{aligned} \quad (15)$$

This integration may be carried out exactly, but the result is rather difficult to interpret. A considerable simplification can be made with very little loss in accuracy as follows: The major contribution to the integral occurs for  $z$  near unity. Since in metals  $l'$  (the mean free path for scattering at energy  $E'$ ) is generally shorter than  $l$  (the mean free path for scattering at the lower energy  $E$ ) and  $x \ln[1 + (1/x)]$  is a very slowly varying function of  $x$  for large  $x$ , very little error is introduced by inserting  $z=1$  in the  $lz/l' \ln[1 + (l'/lz)]$  term of Eq. (15). Under this approximation, Eq. (15) becomes

$$\begin{aligned} R''(E', E) dE dE' &= \frac{KC(E) \dot{p}_2 dEG_0(E') dE'}{\alpha + 1/l} \\ &\quad \times \frac{1}{2} \left[ \frac{1}{\alpha l'} \ln(1 + \alpha l') + \frac{l}{l'} \ln\left(1 + \frac{l'}{l}\right) \right]. \end{aligned} \quad (16)$$

The total rate of escape of electrons with energy between  $E$  and  $E+dE$  after scattering once is Eq. (16) integrated over all  $E'$ .

$$\begin{aligned} R''(E) dE &= \frac{KC(E) dE}{\alpha + (1/l)} \int_E^{\infty} \frac{1}{2} \left[ \frac{1}{\alpha l'} \ln(1 + \alpha l') \right. \\ &\quad \left. + \frac{l}{l'} \ln\left(1 + \frac{l'}{l}\right) \right] \dot{p}_2 G_0(E') dE'. \end{aligned} \quad (17)$$

Note that if  $\alpha l'$  and  $l'/l$  are much smaller than unity, Eq. (17) simplifies to

$$R''(E) dE = \frac{KC(E) dE}{\alpha + (1/l)} \int_E^{\infty} \dot{p}_2 G_0(E') dE'. \quad (18)$$

Combining Eqs. (7) and (17), the rate of escape of electrons with energy between  $E$  and  $E+dE$ , considering only electrons which do not scatter and those which scatter once, is

$$\begin{aligned} R(E) dE &= \frac{KC(E) dE}{\alpha + (1/l)} \left[ G_0(E) + \int_E^{\infty} \frac{1}{2} \left[ \frac{1}{\alpha l'} \ln(1 + \alpha l') \right. \right. \\ &\quad \left. \left. + \frac{l}{l'} \ln\left(1 + \frac{l'}{l}\right) \right] \dot{p}_2 G_0(E') dE' \right]. \end{aligned} \quad (19)$$

The expression given in Eq. (17) for the rate of escape of electrons after scattering once is easily interpreted. The  $(l/l') \ln[1 + (l'/l)]$  term represents those electrons initially excited to energy  $E'$  which are moving away from the photoemitting surface. These electrons eventually will be scattered regardless of the value of the mean free path for scattering, and their probability of escaping after scattering once will depend on the ratio of the mean free paths  $l'/l$ . This shows that inelastic scattering will affect photoemission data even when  $l$  is much longer than the optical absorption depth. The  $(1/\alpha l') \ln(1 + \alpha l')$  term represents those electrons initially excited to energy  $E'$  which

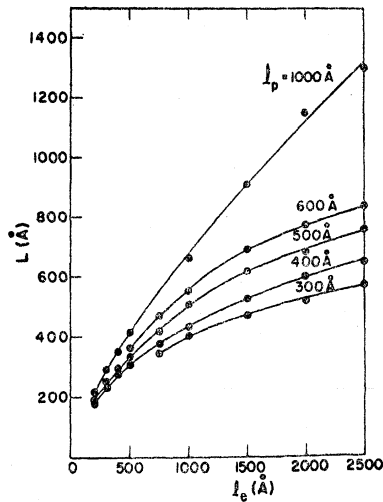


FIG. 4. Attenuation length  $L$  calculated using the Monte Carlo method.  $l_e$  is the electron-electron mean free path and  $l_p$  is the electron-phonon mean free path (after Stuart, Wooten, and Spicer).

are moving toward the photoemitting surface. The probability of these electrons escaping after scattering once will depend on the probability of their scattering once before reaching the surface. If  $l' \gg 1/\alpha$ , most of these electrons will escape without scattering. If  $l' \ll 1/\alpha$ , few will escape without scattering.

### C. Effect of Elastic Scattering

It has been assumed in the previous sections that the mean free path for inelastic scattering is much shorter than the mean free path for elastic scattering. However, in copper and silver electron-phonon interaction is a moderately strong scattering mechanism. This scattering process involves an energy loss small enough compared to the resolution of photoemission measurements that the process may be considered as elastic. An estimate of the energy loss per collision can be obtained in the following way: In a phonon collision, a phonon is either absorbed or emitted with probability proportional to  $n$  and  $n+1$ , respectively, where  $n$  is the equilibrium density of phonons in the metal. Assuming the phonon energy corresponds to the Debye temperature ( $\approx 0.03$  eV in Cu, and  $\approx 0.02$  eV in Ag),<sup>6</sup> the energy loss per collision can be averaged over emission and absorption according to the probabilities involved, phonon emission corresponding to an electron energy decrease equal to the phonon energy, and phonon absorption corresponding to an electron energy increase of the same magnitude. In copper and silver at 300°K, the average energy loss per collision is  $\approx 0.016$  and  $\approx 0.0075$  eV, respectively. These values justify the approximation that phonon collisions are lossless.

The process of electron escape from a photoemitter when the mean free path for elastic scattering is comparable to that for inelastic scattering is difficult to describe exactly in closed mathematical form. However,

<sup>6</sup> C. Kittel, *Introduction to Solid State Physics* (John Wiley & Sons, Inc., New York, 1960).

it has been found both experimentally and theoretically that the probability of escape of an electron with energy  $E$  a distance  $x$  from the surface of a photoemitter can be approximated in this case by<sup>7</sup>

$$p_{\text{esc}}(E, x) = B(E)e^{-x/L}, \quad (20)$$

where  $B(E)$  is a function which takes into account the threshold, and  $L$  is an attenuation length which depends on the mean free paths for inelastic and elastic collisions. Using Eq. (20), calculations similar to those resulting in Eq. (7) give

$$R(E)dE = \frac{B(E)G_0(E)dE}{\alpha + (1/L)}. \quad (21)$$

Stuart, Wooten, and Spicer<sup>8</sup> have used the Monte Carlo method to determine  $L$  for various values of the mean free paths. Some of their results are shown in Fig. 4. In copper and silver, the absorption coefficient is of the order of  $5 \times 10^6 \text{ cm}^{-1}$  in the visible and ultraviolet,<sup>9</sup> and the mean free paths for phonon scattering are approximately 500 Å at the Fermi energy.<sup>10</sup> Even allowing for the fact that the mean free path for elastic scattering at high-electron energies may be somewhat lower than the mean free paths for phonon scattering at the Fermi energy, Fig. 4 indicates that  $1/L$  will be small compared to  $\alpha$  in copper and silver for inelastic collision mean free paths longer than approximately 500 Å. When the mean free path for inelastic collisions is less than 500 Å,  $L$  approaches the value of the inelastic collision mean free path. For these reasons, in copper and silver Eq. (7) may be used as a good approximation over the entire range of electron energies to be studied, if the small effect of elastic collisions is included in the threshold function  $C(E)$ .

### D. Relation of Electron Energy Distribution to Optical Transition Probabilities

The absorption coefficient of a solid  $\alpha$  at frequency  $\nu$  may be defined as

$$\alpha(\nu) = \int_0^\infty \alpha'_\nu(E)dE, \quad (22)$$

if all photons corresponding to frequency  $\nu$  are absorbed in exciting electrons in the solid to higher energy states. In Eq. (22),  $\alpha'_\nu(E)dE$  is the part of  $\alpha(\nu)$  due to electronic transitions to energy states between  $E$  and  $E+dE$ . If  $n_p$  is the flux of photons at frequency  $\nu$  per unit area absorbed by the photoemitting material, then  $G(E, x) \times dEdx$  in Eq. (3) due to optically excited electronic

<sup>7</sup> W. E. Spicer, *J. Appl. Phys.* **31**, 2077 (1960).

<sup>8</sup> R. N. Stuart, F. Wooten, and W. E. Spicer, *Phys. Rev. Letters* **10**, 1-3 (1963); R. N. Stuart, F. Wooten, and W. E. Spicer, *Phys. Rev.* **135**, A495 (1964).

<sup>9</sup> H. Ehrenreich and H. R. Philipp, *Phys. Rev.* **128**, 1622 (1962).

<sup>10</sup> C. Kittel, *Elementary Solid State Physics* (John Wiley & Sons, Inc., New York, 1962), p. 112.

transitions is

$$G(E, x) dE dx = n_p \alpha_\nu'(E) dE e^{-\alpha(\nu) x} dx. \quad (23)$$

This defines  $G_0(E)$  in Eq. (3) as  $n_p \alpha_\nu'(E)$ . Substituting this  $G_0(E)$  in Eq. (19), the number of electrons per absorbed photon at frequency  $\nu$  emitted with energy between  $E$  and  $E + dE$  is

$$\begin{aligned} N(E) dE &= \frac{R(E) dE}{n_p} \\ &= \frac{KC(E) dE}{\alpha + (1/l)} \left( \alpha_\nu'(E) + \int_E^\infty \frac{1}{2} \left[ \frac{1}{\alpha l'} \ln(1 + \alpha l') \right. \right. \\ &\quad \left. \left. + \frac{l}{l'} \ln \left( 1 + \frac{l'}{l} \right) \right] p_{2\alpha_\nu'}(E') dE' \right). \quad (24) \end{aligned}$$

The transition probability per second per unit volume for electrons with energy  $E_0$  in a solid in the presence of an electromagnetic field at frequency  $\nu$  can be determined using first and/or second-order time-dependent perturbation theory if the wave functions in the solid are known. Assume that this probability is  $N_T(E, E_0, \nu)$ , where  $E$  is the energy of the electron after excitation,  $E_0$  is its initial energy, and  $\nu$  is the frequency of the electromagnetic field. Since conservation of energy requires that  $E = E_0 + h\nu$ ,  $N_T$  is not an independent function of both  $E_0$  and  $E$ . The power absorbed per unit volume by the solid is then

$$P = h\nu \int_0^\infty N_T(E, E_0, \nu) dE. \quad (25)$$

Remembering that the conductivity  $\sigma(\nu)$  is defined at optical frequencies in terms of the absorption of power per unit volume,  $\sigma \mathcal{E}_0^2 / 2$ , where  $\mathcal{E}_0$  is the amplitude of the electric vector of the field,

$$\sigma(\nu) = \frac{2h\nu}{\mathcal{E}_0^2} \int_0^\infty N_T(E, E_0, \nu) dE. \quad (26)$$

The absorption coefficient of a solid  $\alpha$  is defined in terms of the conductivity

$$\alpha(\nu) = \sigma(\nu) / n(\nu) c \epsilon_0, \quad (27)$$

where  $n$  is the index of refraction,  $c$  is the velocity of light in free space, and  $\epsilon_0$  is the permittivity of free space. Using Eqs. (26) and (27)

$$\alpha(\nu) = \frac{2h\nu}{n(\nu) c \epsilon_0 \mathcal{E}_0^2} \int_0^\infty N_T(E, E_0, \nu) dE. \quad (28)$$

Comparing Eq. (26) to Eq. (20)

$$\alpha_\nu'(E) = \frac{2h\nu}{n(\nu) c \epsilon_0 \mathcal{E}_0^2} N_T(E, E_0, \nu). \quad (29)$$

It is evident from Eqs. (29) and (24) that if the

electrons that escape without scattering with significant energy loss can be separated from those which escape after scattering with significant energy loss, the energy distribution of the photoemitted electrons at various photon energies can be used to gain a great deal of information on transition probabilities, including selection rules and densities of states. As an example, consider the special case where  $\alpha \gg 1/l$  and, under the assumptions made here, there is a negligible number of electrons which scatter with significant energy loss before escaping. In this case, Eq. (24) becomes

$$N(E) dE = C(E) \alpha_\nu'(E) dE / \alpha(\nu), \quad (30)$$

since  $K$  from Fig. 2 is unity for large  $\alpha l$ . Substituting Eqs. (28) and (29)

$$N(E) dE = C(E) N_T(E, E_0, \nu) dE / \int_0^\infty N_T(E, E_0, \nu) dE. \quad (31)$$

It should be noted that Eq. (31) was derived assuming that only inelastic scattering can take place. Clearly, as  $l$  becomes large, elastic scattering will become important. An important effect of this will be the scattering of electrons into the escape cone.<sup>8</sup> This could be taken into account approximately by redefining  $C(E)$  so that the electrons elastically scattered in the escape cone are considered. In regions away from the threshold where  $C(E)$  is independent of  $E$ , relative values of  $N_T(E, E_0, \nu)$  may be obtained from Eq. (31) without difficulty; however, near the threshold,  $C(E)$  may be a strong function of energy and introduce considerable inaccuracies into the determination of  $N(E)$ .

## E. Effect of Inelastic Scattering on the Energy Distribution of Photoemitted Electrons

### 1. Introduction

The distribution in energy of photoemitted electrons is similar to the distribution in energy of electrons in the solid after optical excitation. However, the distribution is modified by inelastic scattering since the electrons must move through the solid to the photoemitting surface before escaping into vacuum. It is useful to identify three characteristic modifications of photoemission data which are produced by scattering. First, there is scattering of electrons out of the states into which they were optically excited. This effect is taken into account by the term  $1/\{\alpha + [1/l(E)]\}$  in Eq. (24). Since  $l(E)$  normally decreases in metals as energy  $E$  increases, this mechanism will result in a distortion of the energy distributors. A second modification that may occur is that due to lifetime broadening. A third possible modification can be produced by the escape of once-scattered electrons. Such electrons may have been either scattered to lower energies from excited states, or scattered to higher energies from states below the Fermi surface. The contribution of the once-scattered electrons to the photoemission data must be

determined before a detailed analysis of photoemission measurements can be made.

## 2. Electron-Electron Scattering

An important inelastic-scattering mechanism in metals is electron-electron scattering. Motizuki and Sparks<sup>11</sup> have calculated the probability per second of an electron in state  $(E', k')$  being scattered to state  $(E, k)$  by electron-electron scattering, and exciting an electron in state  $(E_0, k_0)$  to state  $(E_1, k_1)$

$$P = (2\pi/\hbar) |\langle k', k_0 | H_{sr} | k, k_1 \rangle|^2 \times \delta[(E' - E) - (E_1 - E_0)]. \quad (32)$$

$H_{sr}$  is the perturbation Hamiltonian applicable to the electron-electron scattering process. To find the total probability per second of an electron with energy  $E'$  being scattered to any other energy  $E$ , Eq. (32) must be summed over all possible states corresponding to  $k', k_0, k, k_1, E, E_1$ , and  $E_0$ . This summation may be carried out if the wave functions and selection rules are known. However, in general this information is not available in enough detail to allow accurate calculations and approximations must be made. Here, it will be assumed that the matrix element in Eq. (32) is independent of the  $k$  vectors of the electrons involved, and has a value represented by  $M_s$ . Such an assumption will allow a relatively uncomplicated examination of the effects of electron-electron scattering on the energy distribution of photoemitted electrons. In the following paper,<sup>12</sup> experimental data from Cu and Ag will be presented and analyzed, and it will be shown that this is a good first-order approximation.

Under the approximation that the matrix element in Eq. (32) is independent of the  $k$  vectors of the electrons involved, the summation described above can be changed to an integral by including the appropriate densities of states and Fermi functions in the standard way. Using this approach, the probability per second of an electron with energy  $E'$  being scattered to an energy between  $E$  and  $E+dE$  is

$$p_s(E', E)dE = \int_0^\infty \left\{ \frac{2\pi}{\hbar} |M_s|^2 \rho(E)\rho(E_0) \times \rho(E_0 + E' - E)F(E_0)[1 - F(E_0 + E' - E)] \times [1 - F(E)]dE \right\} dE_0, \quad (33)$$

where  $|M_s|^2$  is the squared matrix element in Eq. (32),  $F(E)$  is the Fermi function,  $\rho(E)$  is the density of states,

<sup>11</sup> K. Motizuki and M. Sparks, M.L.R. No. 1032, Contract SD-87 (ARPA), W. W. Hansen Laboratories of Physics, Stanford University, California, May 1963 (unpublished).

<sup>12</sup> C. N. Berglund and W. E. Spicer, Phys. Rev. **136**, A1044 (1964), following paper.

and the variable  $E_1$  has been removed using the energy delta function in Eq. (32). Defining

$$g_s(E', E) = \int_0^\infty \frac{2\pi}{\hbar} |M_s|^2 \rho(E_0)\rho(E_0 + E' - E)F(E_0) \times [1 - F(E_0 + E' - E)]dE_0, \quad (34)$$

Eq. (33) becomes

$$p_s(E', E)dE = \rho(E)[1 - F(E)]g_s(E', E)dE \quad (35)$$

and the total probability per second of an electron with energy  $E'$  being scattered to any energy is

$$P_s(E') = \int_0^\infty p_s(E', E)dE. \quad (36)$$

Note that this probability  $P_s(E')$  is the reciprocal of the lifetime  $\tau(E')$  for electron-electron scattering of an electron with energy  $E'$ . If a group velocity  $v_g(E')$  is defined which applies to electrons of energy  $E'$ , the mean free path for electron-electron scattering  $l(E')$  is given by

$$l(E') = v_g(E')\tau(E') = v_g(E')/P_s(E'). \quad (37)$$

Given that an electron with energy  $E'$  suffers an electron-electron scattering event, the probability  $p_2$  of its scattering to a lower energy between  $E$  and  $E+dE$  must be

$$p_2 = p_s(E', E)dE/P_s(E'). \quad (38)$$

In addition to the scattering of an energetic electron down to an energy between  $E$  and  $E+dE$  included in Eq. (38), there is also the scattering of an electron from a state below the Fermi level which must be included in  $p_2$ . Fortunately, this scattering effect can be included in  $p_2$  in a simple way. Figure 5 shows the two processes that may occur in an electron-electron scattering event involving the four electronic states in Eq. (32). Both processes result in an electron with energy  $E$ , but in one case the electron has been scattered from a higher energy  $E'$ , and in the other case it has been scattered from a state below the Fermi level. It can easily be shown that the probability of the two processes are equal. Hence, the excitation of electrons from states below the Fermi level by the scattering can be included

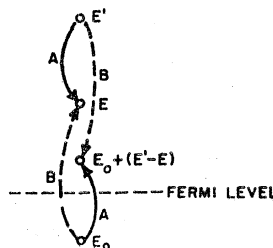


FIG. 5. Two possible electron-electron scattering processes, A and B, involving four electronic states.

by using

$$p_2 = 2p_s(E', E)dE/P_s(E'). \quad (39)$$

Substituting Eq. (39) in Eq. (24)

$$N(E)dE = \frac{KC(E)dE}{\alpha + (1/l)} \left[ \alpha_v'(E) + 2 \int_E^\infty \frac{1}{2} \frac{1}{\alpha l'} \ln(1 + \alpha l') + \frac{l}{l'} \ln\left(1 + \frac{l'}{l}\right) \right] \frac{p_s(E', E)}{P_s(E')} \alpha_v'(E') dE'. \quad (40)$$

In many cases,  $\alpha l' \ll 1$ ,  $l'/l \ll 1$  and the Fermi function at absolute zero may be used in the equations. Under these assumptions, Eq. (40) simplifies to

$$N(E)dE = \frac{KC(E)dE}{\alpha + (1/l)} \times \left[ \alpha_v'(E) + 2 \int_E^{E_F + h\nu} \frac{p_s(E', E)}{P_s(E')} \alpha_v'(E') dE' \right], \quad (41)$$

where  $E_F$  is the Fermi energy. Another effect of electron-electron scattering is illustrated by Eq. (41). Due to the factor of 2 before the scattering term, an increase in quantum yield may occur. That is, optically excited energetic electrons may scatter once before escaping, exciting a second electron from a state below the Fermi level which may also escape. This may result in a quantum yield greater than unity.

### 3. Plasmon Creation

In Eq. (40), the energy distribution of photoemitted electrons has been calculated assuming that electron-electron scattering is the only important inelastic-scattering mechanism. In some metals, such an assumption may be accurate over a wide range of electron energy. However, in others, electron scattering due to plasmon creation might also be an important inelastic scattering mechanism,<sup>13</sup> and Eq. (40) must be modified to include this scattering.

The derivation of an expression for the energy distribution of photoemitted electrons including both electron-electron scattering and scattering by plasmon creation is relatively straightforward. Such an expression illustrates in detail the effects of the scattering mechanisms. However, the effects of scattering by plasmon creation can be illustrated more easily by assuming that plasmon creation is the only important inelastic-scattering mechanism. Since the electron energy loss in a plasmon scattering event must be equal to the plasmon energy  $h\nu_p$ , the probability  $p_2$  in Eq. (24) must be  $\delta(E' - E - h\nu_p)$ . Substituting in Eq. (24), one would obtain

$$N(E)dE = \frac{KC(E)dE}{\alpha + (1/l)} \left[ \alpha_v'(E) + \frac{1}{2} \frac{1}{\alpha l'} \ln(1 + \alpha l') + \frac{l}{l'} \ln\left(1 + \frac{l'}{l}\right) \right] \alpha_v'(E + h\nu_p). \quad (42)$$

<sup>13</sup> J. J. Quinn, Phys. Rev. 126, 1453 (1962).

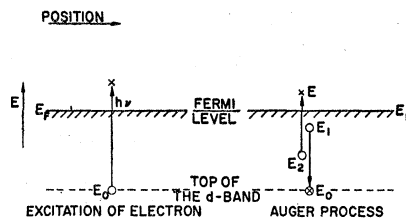


FIG. 6. Illustration of the Auger process in a metal.

Equation (42) indicates that strong scattering by plasmon creation would result in a once-scattered contribution to energy distribution curves of the same general shape as the contribution of electrons which escaped without scattering, but shifted to lower energy by the plasmon energy  $h\nu_p$ . In practice, the magnitude of the once-scattered contribution due to scattering by plasmon creation would not be given by Eq. (42), but would depend on the mean free paths for electron-electron scattering and scattering by plasmon creation. However, it is evident from Eq. (42) that the effect of scattering by plasmon creation would be relatively easy to identify in curves of the energy distribution of photoemitted electrons if the scattering process were strong.

### F. Effects of the Auger Process on the Energy Distribution of Photoemitted Electrons

In order to fully discuss the effects of scattering on photoemission data from metals, the Auger process must be considered.<sup>14</sup> This process in a metal is illustrated in Fig. 6. An electron is excited from a state at energy  $E_0$  leaving a hole. Another electron with energy  $E_1$  larger than  $E_0$  recombines with this hole. A third electron, initially having energy  $E_2$ , absorbs the energy released ( $E_1 - E_0$ ) and is excited into a state above the Fermi level at energy  $E$ . For conservation of energy,

$$E - E_2 = E_1 - E_0. \quad (43)$$

If the energy  $E$  of the excited electron is large enough, the electron may escape into vacuum and appear as a photoelectron. It should be noted that the Auger process is the inverse of the event in which an energetic electron is scattered to lower energy by means of an electron-electron interaction. As a result, it can be treated in a similar way.

Consider the process illustrated in Fig. 6 as the scattering of an energetic hole. The probability per second of a hole with energy  $E_0$  producing an electron with energy between  $E$  and  $E + dE$  through the Auger process may be written, analogous to Eq. (33) for

<sup>14</sup> See, for instance, H. D. Hagstrum, Phys. Rev. 96, 336 (1954).



electron-electron scattering, as

$$p_a(E_0, E) dE = \int_0^\infty \left\{ \frac{2\pi}{\hbar} |M_a|^2 \rho(E) \rho(E_1) \right. \\ \left. \times \rho(E+E_0-E_1) F(E_1) F(E+E_0-E_1) \right. \\ \left. \times [1-F(E)] dE \right\} dE_1, \quad (44)$$

where  $|M_a|^2$  is the squared matrix element applicable to the process and  $F(E)$  is the Fermi function. Defining

$$g_a(E_0, E) = \int_0^\infty \frac{2\pi}{\hbar} |M_a|^2 \rho(E_1) \rho(E+E_0-E_1) \\ \times F(E_1) F(E+E_0-E_1) dE_1, \quad (45)$$

Eq. (44) becomes

$$p_a(E_0, E) dE = \rho(E) [1-F(E)] g_a(E_0, E) dE \quad (46)$$

and the total probability per second of a hole with energy  $E_0$  being involved in the Auger process is

$$P_a(E_0) = \int_0^\infty p_a(E_0, E) dE. \quad (47)$$

Following the derivation given for electron-electron scattering, it can easily be shown that the contribution by the Auger process to the number of electrons which escape from a photoemitter with energy between  $E$  and  $E+dE$  is

$$N_a(E) dE = \frac{KC(E) dE}{\alpha + (1/l)} \int_0^\infty \left[ \frac{1}{2} \ln(1 + \alpha l_0) \right. \\ \left. + \frac{l}{l_0} \ln \left( 1 + \frac{l_0}{l} \right) \right] \frac{p_a(E_0, E)}{P_a(E_0)} \alpha'_v(E_0 + h\nu) dE_0, \quad (48)$$

where  $l_0$  is the mean free path for the Auger process for holes of energy  $E_0$ . This expression simplifies somewhat when  $\alpha l_0 \ll 1$ ,  $(l_0/l) \ll 1$ , and the Fermi function at absolute zero applies.

$$N_a(E) dE = \frac{KC(E) dE}{\alpha + (1/l)} \\ \times \int_0^{E_F - (E - E_F)} \frac{p_a(E_0, E)}{P_a(E_0)} \alpha'_v(E_0 + h\nu) dE_0. \quad (49)$$

It may be useful here to combine Eqs. (49) and (41) to obtain an expression for the energy distribution of photoemitted electrons when electron-electron scattering is the dominant scattering process for energetic electrons and the Auger process is the dominant scattering process for energetic holes.

$$N(E) dE = \frac{KC(E) dE}{\alpha + (1/l)} \\ \times \left[ \alpha'_v(E) + 2 \int_E^{E_F + h\nu} \frac{p_s(E', E)}{P_s(E')} \alpha'_v(E') dE' \right. \\ \left. + \int_0^{E_F - (E - E_F)} \frac{p_a(E_0, E)}{P_a(E_0)} \alpha'_v(E_0 + h\nu) dE_0 \right]. \quad (50)$$

A more complex expression will, of course, result if scattering by plasmon creation is also included.

### III. THE QUANTUM YIELD

The quantum yield is defined as the total number of electrons which escape from a photoemitter per absorbed quantum at a given photon energy. Hence,

$$Y(\nu) = \int_{E_w}^\infty N(E) dE, \quad (51)$$

where  $E_w$  is the energy corresponding to the Fermi energy plus the work function, i.e., the energy at the vacuum level. In general, the quantum yield per incident photon  $Y'(\nu)$  is measured for a material. This is related to the yield per absorbed photon through the reflectivity  $R_e(\nu)$

$$Y(\nu) = Y'(\nu) / [1 - R_e(\nu)]. \quad (52)$$

The spectral dependence of the quantum yield near the threshold for photoemission has been considered in great detail in the literature.<sup>1,3</sup> However, at photon energies well above threshold, the quantum yield has only recently been considered.<sup>15</sup> The quantum yield at these photon energies is of interest because it can be used to verify interpretations of the electron energy distributions, and also to gain information concerning the band structure between the Fermi level and the vacuum level. To illustrate this point, assume that the scattering term in Eq. (24) is negligible, i.e.,  $l \gg 1/\alpha$ , and  $C(E)$  is a step function equal to a constant for electron energies greater than  $E_w$ . Following Spicer,<sup>16</sup> define  $\alpha_a(\nu)$  as that part of the absorption coefficient at frequency  $\nu$  associated with transitions to states above the vacuum level, and  $\alpha_b(\nu)$  as that part of the absorption coefficient at frequency  $\nu$  associated with transitions to states between the Fermi level and the vacuum level. Then the quantum yield is given by

$$Y(\nu) \propto \alpha_a(\nu) / [\alpha_a(\nu) + \alpha_b(\nu)]. \quad (53)$$

It can be seen that transitions to states between the Fermi level and the vacuum level affect the yield through  $\alpha_b(\nu)$  in the denominator of Eq. (53). An excellent example of this is the yield minimum in silicon at 4.4 eV due to the occurrence of very strong transitions to states below the vacuum level at that photon energy.<sup>17</sup>

### IV. INTERPRETATION OF PHOTOEMISSION MEASUREMENTS

#### A. Direct and Nondirect Transitions

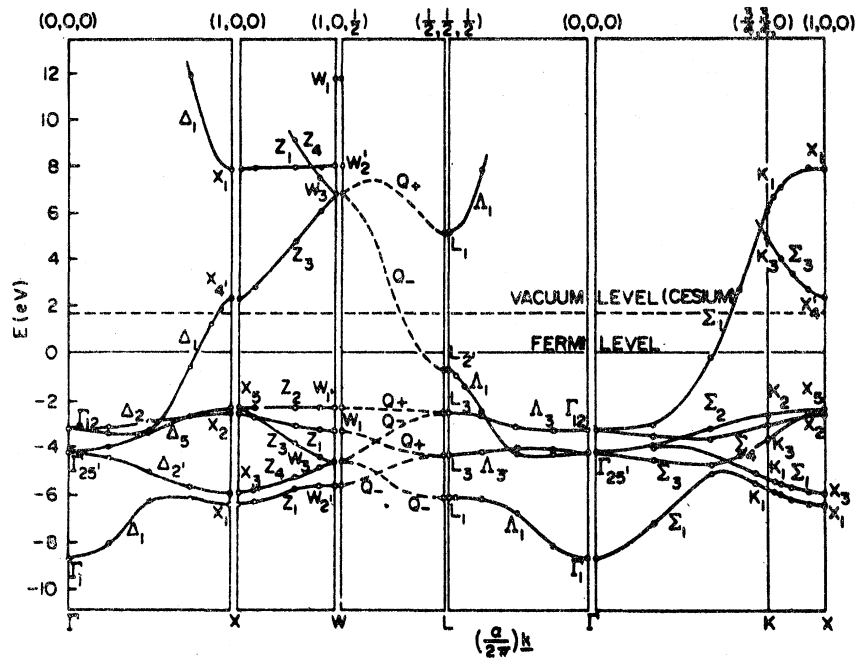
From photoemission measurements, it can be established whether nondirect or direct optical transitions

<sup>15</sup> W. E. Spicer, Phys. Rev. **112**, 114 (1958); W. E. Spicer, Phys. Chem. Solids **22**, 365 (1961).

<sup>16</sup> W. E. Spicer, J. Appl. Phys. **31**, 2077 (1960).

<sup>17</sup> W. E. Spicer and R. E. Simon, Phys. Rev. Letters **9**, 385 (1962).

FIG. 7. Calculated band structure of copper (after Segall).



are most important in a solid. Transitions in which direct conservation of  $k$  vector is important will be referred to here as direct transitions, and all others as nondirect. In the following paper, experimental data from copper and silver will be presented and discussed. As a result, it will be most fruitful here to focus our attention on a hypothetical material whose band structure we will assume to be completely defined by the  $E$  versus  $k$  diagram calculated along the principal directions of copper, and to illustrate using this band structure the different effects on photoemission data of direct and nondirect transitions. In the following article, the actual experimental data will be examined, and the theoretical significance of nondirect transitions will be discussed.

All analysis of experimental data is based on the assumption that structure in the optical transition probability centered at a given final energy will produce corresponding structure in the energy distribution of the emitted electrons. For this to occur, a representative sample of the excited electrons must escape. The structure in the optical transition probability may be associated with a critical point in the final states. Since  $\nabla_k \mathcal{E} \rightarrow 0$  at the critical point, the group velocity of these electrons will be zero. Of course, finite group velocity is a requirement for emission. This problem must be examined in detail. It is unimportant, to the first approximation, if the critical point is a band maximum or minimum since the number of available final states will go to zero at the critical point. However, if the critical point is a saddle point, the situation may be more serious. Two factors, must be considered. First, what fraction of the electrons associated with the peak

in the final density of states are excited to states with  $\nabla_k \mathcal{E} = 0$  and what fraction have small but finite group velocities. Second, of the electrons with insufficient group velocities to escape, what fraction will suffer scattering with large energy loss (electron-electron scattering) and what fraction will suffer scattering with negligible energy loss (scattering due to phonons, imperfections, etc.). In the former case, the electrons will not appear in the original distribution and information concerning the optical transition probability will be lost; however, in the second case the electrons may be scattered into states with group velocity sufficiently large to allow escape. In the latter case, the information on the optical transition probability will be retained. A quantitative treatment of these effects is not possible here. However, it is clear that a peak in the distribution of emitted electrons may result from optical transitions to a saddle point even though the relative magnitude of this peak may be reduced. Very strong peaks in the energy distribution from silicon have been observed where the final state was a saddle point. The best example is the transition to the  $L_3$  point. A very strong maximum has been observed experimentally in the energy distributions<sup>17,18</sup> corresponding to this transition in good agreement with calculations from band theory.<sup>18-20</sup> In making detailed comparison between theory and experiment, Brust<sup>18,20</sup> found no evidence for a reduced escape probability for the electrons excited to the saddle point.

<sup>18</sup> D. Brust, Bull. Am. Phys. Soc. 9, 274 (1964).

<sup>19</sup> D. Brust, M. L. Cohen, and J. C. Phillips, Phys. Rev. Letters 9, 389 (1962).

<sup>20</sup> D. Brust, Phys. Rev. 134, A1337 (1964).

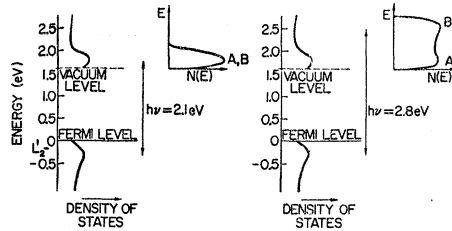


FIG. 8. Illustration of nondirect transitions in a metal.

The calculated band diagram for copper is shown in Fig. 7. The vacuum level marked on the diagram is the vacuum level which results when approximately a monolayer of cesium is placed on the surface of copper. The relatively flat bands lying 2 eV or more below the Fermi surface are associated principally with *d* atomic levels whereas the bands lying at higher energy are associated principally with *s* and *p* atomic levels.

Consider first the *s*- and *p*-like states just below the Fermi level and just above the vacuum level. When the photon energy is less than the energy difference between  $L_2'$  and  $L_1$  (approximately 4 eV), only nondirect transitions can affect the photoemission results. Because of this, the transition probabilities involved will be, to the first approximation, proportional to the product of the initial and final density of states. Since the saddle points at  $X_4'$  and  $L_2'$  correspond to peaks in the density of states, it is expected that strong transitions will occur from states near  $L_2'$ , and strong transitions will occur to states near  $X_4'$ . Figure 8 shows the energy distribution of photoemitted electrons to be expected in this case at two photon energies when only nondirect transitions need be considered. The significant characteristic of nondirect transitions is that a peak in the energy distribution of photoemitted electrons due to such transitions either (1) remains located at a constant energy in the distribution as photon energy is changed, the energy of such a peak corresponding to the location of a maximum in the final density of states (peak A in Fig. 8), or (2) moves to higher energy in increments equal to the change in photon energy, corresponding to a maximum in the initial density of states (peak B in Fig. 8).

The peak in the energy distributions due to the peak in the density of states at  $L_2'$  (peak B) shown in Fig. 8 will continue to move to higher energy as photon energy is increased, the energy at the peak,  $E_p$ , being given by the equation

$$E_p = E_i + h\nu, \quad (54)$$

where  $E_i$  is the energy at the symmetry point  $L_2'$ . However, when the photon energy becomes greater than the energy difference between  $L_1$  and  $L_2'$  in Fig. 7, direct transitions will be allowed from states near  $L_2'$  to states near  $L_1$ , and these transitions will also contribute to photoemission data. In Fig. 9, the peak contributed to the energy distribution of photoemitted electrons by

direct transitions between states near  $L_2'$  and states near  $L_1$  is indicated for several photon energies. At  $h\nu$ , no direct transitions are allowed; at  $h\nu_1$ , the photon energy just equals the energy difference between  $L_1$  and  $L_2'$ , and there is a contribution by direct transitions; at  $h\nu_3$  and  $h\nu_4$ , the peak is larger, and is being excited to higher energy. The important feature of the peak due to direct transitions illustrated in Fig. 9 is that the peak moves to higher energy as photon energy is increased at a somewhat slower rate than that given by Eq. (54). This occurs because the energy of the initial states responsible for the peak is a function of photon energy. It is this characteristic of peaks due to direct transitions that allows one to establish unambiguously from photoemission data the relative strength of non-direct and direct transitions in a solid.

A second example of the interpretation of photoemission measurements in terms of direct and nondirect transitions is given by transitions from the *d* bands of copper. Consider the excitation of *d* electrons to states near  $X_4'$  in the band structure (see Fig. 7). Figure 10 shows the contribution to the energy distribution of photoemitted electrons at two photon energies  $h\nu_1$  and  $h\nu_2$  due to direct transitions. It is noted that the peak due to direct transitions from the top *d* band (labeled A) moves to higher energy in increments approximately equal to the change in photon energy, i.e., follows the relation given by Eq. (54). This occurs because the *d* band is approximately "flat," and one cannot tell from photoemission measurements the difference between direct transitions to or from flat bands and nondirect transitions. (This will be discussed in detail later.) However, the peaks due to transitions from the other *d* bands (labeled B and C) do not follow Eq. (54) because they are not flat. The energies of the initial states responsible for the peaks decrease as photon energy increases.

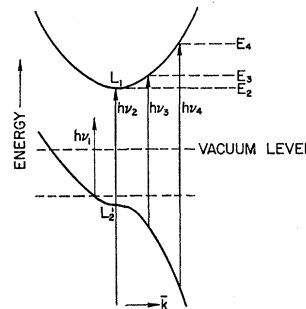
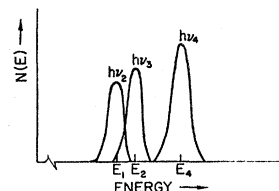


FIG. 9. Direct transitions in copper and their contribution to photoemission. Note that  $E_3 - E_2 = h\nu_3 - h\nu_2$  and  $E_4 - E_3 = h\nu_4 - h\nu_3$ .



Now consider the contribution to photoemission data of nondirect transitions from the *d* bands to states near  $X_4'$ . For nondirect transitions, the transition probabilities will reflect the density of states, and the energy distribution at two photon energies will be similar to those in Fig. 11. Peaks in the energy distribution of photoemitted electrons due to peaks in the *d*-band density of states will move to higher energy in increments equal to the change in photon energy, and a peak due to the peak in the density of states at  $X_4'$  will remain at a constant energy independent of photon energy.

The above examples illustrate how the contribution of direct and nondirect transitions to photoemission data can be separated, and how this information can be used to determine the relative strength of direct and nondirect transitions. Spicer and co-workers have used photoemission with considerable success to determine, for instance, that direct conservation of *k* vector is important for optically excited transitions in silicon,<sup>17</sup> but not in Cs<sub>3</sub>Sb and Cs<sub>3</sub>Bi.<sup>5,21</sup>

**B. Effect of Electron-Scattering Processes**

It has been mentioned that strong scattering processes result in lifetime broadening of absorption peaks, and also distort the energy distribution of photoemitted electrons due to the  $1/[\alpha + 1/l(E)]$  term in Eq. (24). In addition to these effects, electrons sometimes escape after scattering and contribute to the energy distributions. It is important to identify the electrons which escape after scattering in order to take the effect of scattering into account in determining band structure from photoemission data. It is also possible to identify the scattering mechanism or mechanisms which are dominant in a solid, and determine some scattering

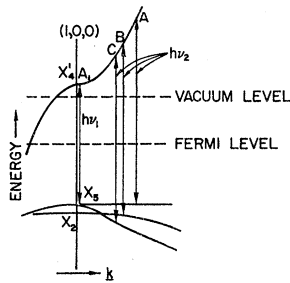
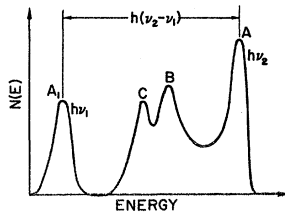


FIG. 10. Energy distributions to be expected for direct optical transitions from the *d* band of copper.



<sup>21</sup> E. A. Taft and H. R. Philipp, Phys. Rev. **115**, 1583 (1959).

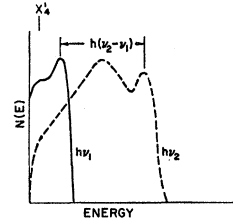


FIG. 11. Energy distributions to be expected for nondirect optical transitions from the *d* band of copper.

parameters. A very simple example will illustrate the effect of electron-electron scattering.

Assume a material in which the density of states is a constant  $\rho_0$  above and below the Fermi level. Also assume that  $|M_s|^2$  in Eq. (33) is independent of electron energies, and the Fermi function at absolute zero applies. Equation (33) then reduces to

$$p_s(E', E)dE = \int_{E_F - (E' - E)}^{E_F} \left( \frac{2\pi}{\hbar} |M_s|^2 \rho_0^3 dE_0 \right) dE_0$$

$$= \frac{2\pi}{\hbar} |M_s|^2 \rho_0^3 (E' - E) dE \tag{55}$$

and Eq. (36) becomes

$$P_s(E') = \int_{E_F}^{E'} \frac{2\pi}{\hbar} |M_s|^2 \rho_0^3 (E' - E) dE$$

$$= \frac{\pi}{\hbar} |M_s|^2 \rho_0^3 (E' - E_F)^2 dE, \tag{56}$$

where  $E_F$  is the Fermi energy. If  $\alpha'_v(E)$  is a constant  $\alpha'_v$  independent of electron energy, and if it is assumed that  $\alpha'_l$  and  $l'/l$  are much smaller than unity, Eq. (40) becomes

$$N(E)dE = \frac{KC(E)\alpha'_v dE}{\alpha + (1/l)}$$

$$\times \left[ 1 + 2 \int_E^{E_F + h\nu} \frac{2(E' - E)}{(E' - E_F)^2} dE' \right]$$

$$= \frac{KC(E)\alpha'_v dE}{\alpha + (1/l)}$$

$$\times \left[ 1 + 4 \left( \frac{E - E_F}{h\nu} - 1 + \ln \frac{h\nu}{E - E_F} \right) \right]. \tag{57}$$

The energy distribution  $N_\nu(E)$  for several photon energies assuming a typical threshold function  $C(E)$  and neglecting  $1/l(E)$  compared to  $\alpha(\nu)$  is shown in Fig. 12. The once-scattered contribution is shaded. The important feature of the figure is that electron-electron scattering results in a low-energy peak in the energy distributions of photoemitted electrons. The position of the peak remains approximately constant

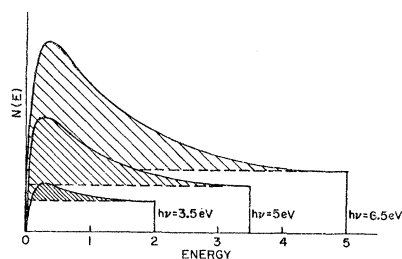


FIG. 12. Theoretical energy distribution of photoemitted electrons for a metal including the effect of electron-electron scattering. The cross-hatched area indicates the contribution due to once-scattered electrons.

in energy just above the vacuum level and the size of the peak increases as photon energy increases.

The above example, although very crude, illustrates the way in which electron-electron scattering affects the energy distribution of photoemitted electrons. Comparison of this simple example to the experimental data of Dickey on Na and K, however, shows how well the simple model predicts the shape and behavior of that part of the electron energy distribution of photoemitted electrons due to once-scattered electrons.<sup>22</sup> Dickey's curves for Na are shown in Fig. 13. The peak in the distributions centered at  $E_m - E = 0.3$  eV is due to transitions from states below the Fermi level. These transitions are apparently nondirect. The remainder of the distribution is due to the contribution of once-scattered electrons as described above. Further verification of the accuracy of the scattering model is given by the results from copper and silver to be presented in the following article.

Silver has a plasma resonance at  $h\nu_p = 3.85$  eV. It

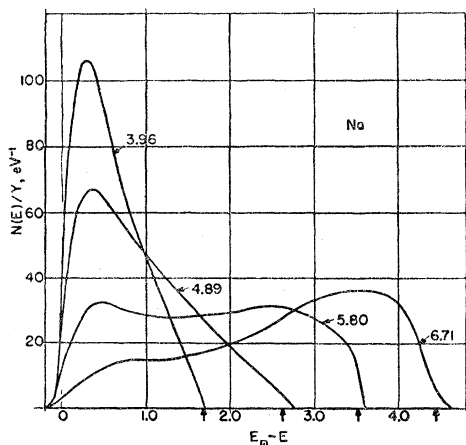


FIG. 13. Energy distribution from K (after Dickey). The energy of the exciting photons is indicated beside each curve. Note that  $E_m - E$  is plotted on the abscissa.  $E_m$  is the maximum energy and  $E$  is the measured energy.

<sup>22</sup> J. Dickey, Phys. Rev. 81, 612 (1951).

might be expected that scattering of electrons with energy more than 3.85 eV above the Fermi level by plasmon creation is a strong scattering mechanism in this metal. Applying directly Eq. (42) with  $\alpha'$  and  $l'/l$  much less than unity, the behavior shown in Fig. 14 for the energy distribution of photoemitted electrons at two photon energies might result. The shaded portion represents those electrons which have scattered once by plasmon creation before escaping. It is a replica of the original distribution reduced in energy by the plasmon energy. It is evident that if this scattering mechanism is important, it will be easily detected by studying the energy distribution curves for silver.

### C. Effects of the Auger Process

It is evident by comparison of Eq. (48) to Eq. (40) that the effects of the Auger process on photoemission data will show marked similarity to those of electron-electron scattering; that is, a low-energy peak will appear in the energy distribution of photoemitted electrons due to the Auger-excited electrons, and an

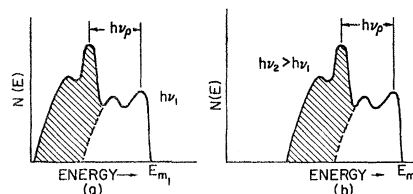


FIG. 14. Effect of scattering by plasmon creation on photoemission. The shaded region represents the contribution of once-scattered electrons.

increase in quantum yield will occur. Because of this, it may often be difficult to determine whether electron-electron scattering or the Auger process is responsible for observed photoemission results. However, in many materials it is possible to separate the two processes unambiguously. One example of a material where this occurs is silver, described in detail in the following article.<sup>12</sup> Another example is sodium, where it is known that the bottom of the filled band is 3 eV below the Fermi level. In this case, the maximum possible energy of an Auger excited electron is 3 eV above the Fermi level. As a result, in photoemission measurements of sodium, any distribution of electrons which extends to an energy more than 3 eV above the Fermi level cannot be due to the Auger process.

### D. The Density of States

In materials where it is found that nondirect transitions are dominant, the density of states can often be determined from photoemission data. The following discussion will illustrate how this may be done,

If transitions are known to be nondirect, the transition probability, neglecting lifetime broadening, when light of photon energy  $h\nu$  is directed onto a solid may be written as the product of the initial and final density of filled and empty states, respectively, and some oscillator strength  $f$ .

$$N_T(E, E_0, \nu) = \mathcal{E}_0^2 f \rho(E_0) \rho(E) F(E_0) [1 - F(E)] \times \delta(E - E_0 - h\nu). \quad (58)$$

Assuming the Fermi function at absolute zero for simplicity, Eq. (58) can be substituted in Eq. (31) to give

$$N(E) dE = \left[ f C(E) \rho(E) \rho(E - h\nu) dE \right] \int_{E_F}^{E_F + h\nu} f \rho(E) \rho(E - h\nu) dE \Big|_{E_F < E < E_F + h\nu}. \quad (59)$$

If  $f$  is assumed independent of electron energy at a given photon energy, Eq. (59) becomes

$$N(E) dE = C(E) \rho(E) \rho(E - h\nu) dE \Big| \int_{E_F}^{E_F + h\nu} \rho(E) \rho(E - h\nu) dE. \quad (60)$$

Equations (59) and (60) show that the energy distribution of photoemitted electrons is proportional to the product of the initial and final density of states. By comparing energy distributions at several photon energies, it is possible to determine the density of states below the Fermi level and above the vacuum level. This technique has been used to determine the density of states of copper and silver, and will be described in more detail later.

In determining the density of states above the vacuum level from photoemission data, the threshold function  $C(E)$  in Eqs. (59) and (60) must be known. In general, this is a complicated function of electron energy, and is not easily determined accurately. However, at electron energies well above threshold it is relative constant, and at electron energies near threshold it can generally be estimated with sufficient accuracy.

The density of states between the Fermi level and the vacuum level cannot be determined directly from the photoemission data. However, an estimate can be made of the density of states in this energy range using Eq. (59) and the measured quantum yield. Assuming a trial density of states between the Fermi level and the vacuum level, and knowing the density of states at other energies and  $C(E)$  from the experimental data,

Eq. (59) can be integrated to give for the yield

$$Y(\nu) = \int_{E_w}^{E_F + h\nu} C(E) f \rho(E) \rho(E - h\nu) dE \Big/ \int_{E_F}^{E_F + h\nu} f \rho(E) \rho(E - h\nu) dE. \quad (61)$$

Since the denominator of Eq. (61) is dependent on the density of states between the Fermi level and the vacuum level, comparison of the calculated yield to the observed yield can be used to determine indirectly the density of states in this energy range.

If scattering is strong so that Eq. (59) is not a good approximation for  $N_\nu(E) dE$ , the density of states is more difficult to determine. In this case, the contribution to the energy distributions of once-scattered electrons and Auger-excited electrons must be estimated, and the mean free path  $l$  as a function of energy be known. However, even if scattering is strong, as in the case of copper and silver, most of the features of the density of states can always be determined from photoemission measurements.

## V. DISCUSSION AND CONCLUSIONS

The analysis of the photoemission process presented has emphasized the characteristics of the phenomena when the photon energy of the incident light is much above threshold. Only those electrons which are excited optically to higher energy states and escape without suffering an inelastic collision, and those electrons which escape after suffering one inelastic collision have been considered. The once-scattered electrons which escape include those scattered from higher energy states, those scattered by electron-electron scattering from states below the Fermi level, and those produced by the Auger process. Using a simple model, expressions for the energy distribution of photoemitted electrons and the quantum yield were derived. These expressions give a remarkable amount of information on the effect of various optical absorption processes and electron-scattering mechanisms on photoemission data, and provide the experimentalist with a basis for interpreting photoemission measurements.

In Sec. IV, detailed descriptions of the effects of various absorption and scattering mechanisms have been given. It has been shown that the contribution to photoemission data of electrons which escape without inelastic scattering can be separated from the contribution of electrons which escape after scattering, and that the data can be used to determine the relative strength of direct and nondirect optically excited transitions in a solid, and to determine the nature and strength of the scattering mechanisms.

It has been mentioned that one cannot tell the difference in photoemission data between direct tran-

sitions to or from flat energy bands and nondirect transitions. However, the resolution of photoemission data is approximately 0.1 eV. Hence, a band would have to vary over less than 0.1 eV before this ambiguity would arise. The five  $d$  bands in copper, for instance, extend over 3.5 eV, so this problem should not be important in this material. In materials where bands

are narrower than 0.1 eV, it is evident that the concepts of direct transitions and Bloch waves lose their importance, since the wave functions are probably represented more accurately in terms of atomic orbitals.

In the following article, photoemission measurements of copper and silver which illustrate most of the effects described here are presented and interpreted.

## Photoemission Studies of Copper and Silver: Experiment\*†

C. N. BERGLUND‡ AND W. E. SPICER

*Stanford Electronics Laboratories, Stanford University, Stanford, California*

(Received 22 June 1964)

Experimental photoemission data from copper and silver are presented and interpreted in detail in terms of the calculated band structures over a photon energy range from 1.5 to 11.5 eV. It is shown that nondirect optical transitions are stronger than direct ones in both metals. In fact, the only direct optical transitions observed are rather weak ones between  $p$ - and  $s$ -like states near  $L_2'$  and  $L_1$  in the calculated band structures. No evidence of direct transitions from the  $d$  bands is found. From the data, the density of states for copper and silver is determined from approximately 7 eV below the Fermi level to approximately 10 eV above it. Several symmetry points in the calculated band structures, and the  $d$  bands, are located absolutely in energy. It is found that electron-electron scattering is the dominant inelastic scattering mechanism for energetic electrons in the metals over the range of energy studied. No evidence of electron scattering by plasmon creation is found. In the silver data, the Auger process is identified, and its effect on photoemission is discussed in detail. To check on the results and conclusions drawn from the photoemission studies, and to illustrate the utility of the method, the spectral distribution of the quantum yield and the energy distribution of photoemitted electrons at several photon energies for copper are calculated and compared to the observations. The contribution of the Auger process to photoemission is calculated and compared to the observations for silver. In addition, the imaginary part of the dielectric constant  $\epsilon_2$  for both copper and silver is calculated, assuming that only nondirect optical transitions are important, and compared to measured values. In all cases, very good agreement is obtained.

### I. INTRODUCTION

IN the previous paper,<sup>1</sup> the effects of different optical transitions and electron scattering processes on photoemission from metals have been described. In this paper, experimental data from the metals copper and silver are presented which illustrate most of these effects. The data are interpreted in detail in terms of the calculated band structures of the metals. In this paper, as in the preceding one, optically excited electronic transitions in which direct conservation of  $k$  vector is not required are referred to as nondirect transitions.

A description of the instrumentation used is given elsewhere.<sup>2</sup> The phototubes used were of the same design as those used by Apker *et al.*,<sup>3</sup> and Spicer.<sup>4</sup> The metals

were evaporated onto the photocathode and collector in vacuum to a thickness of approximately 2000 to 5000 Å. Following evaporation of the metal, approximately a monolayer of cesium was deposited on the surface of the metals to reduce the work function to values of 1.55 and 1.65 eV for copper and silver, respectively. The optimum layer of cesium on the metal surface was determined by maximizing the photoemission from the metal when it was irradiated with light from a tungsten lamp.

In order to verify that the cesium layer had no effect on the photoemission results other than the reduction in work function, a copper phototube was constructed without cesium treatment. The experimental results from this tube were consistent with the results reported here for tubes with cesium on the surface.

### II. PHOTOEMISSION STUDY OF COPPER

#### A. The Calculated Band Structure of Copper

Calculations of the energy band structure of copper have recently been made by Segall and Burdick.<sup>5,6</sup> It is

\* Work supported by the Advanced Research Projects Agency through the Center for Materials Research at Stanford University, Stanford, California.

† Based on a thesis submitted by C.N.B. to Stanford University in partial fulfillment of the requirements of the Ph.D. degree.

‡ Present address: Bell Telephone Laboratories, Murray Hill, New Jersey.

<sup>1</sup> C. N. Berglund and W. E. Spicer, Phys. Rev. **136**, A1030 (1964), preceding paper.

<sup>2</sup> W. E. Spicer and C. N. Berglund (to be published).

<sup>3</sup> L. Apker, E. Taft, and J. Dickey, J. Opt. Soc. Am. **43**, 78 (1953).

<sup>4</sup> W. E. Spicer, Phys. Chem. Solids **22**, 365 (1961).

<sup>5</sup> B. Segall, Phys. Rev. **125**, 109 (1962).

<sup>6</sup> G. A. Burdick, Phys. Rev. **129**, 138 (1963).